Spectroscopic characterization of rare events in colloidal particle stochastic thermodynamics

Sandro K. Otani,[1] Thalyta T. Martins,[2] Sérgio R. Muniz,[2] P.C. de Sousa Filho,[1] Fernando A. Sigoli[1] and René A. Nome[1]

1: Institute of Chemistry, State University of Campinas

2: São Carlos Institute of Physics, University of São Paulo

GRAPHICAL ABSTRACT:

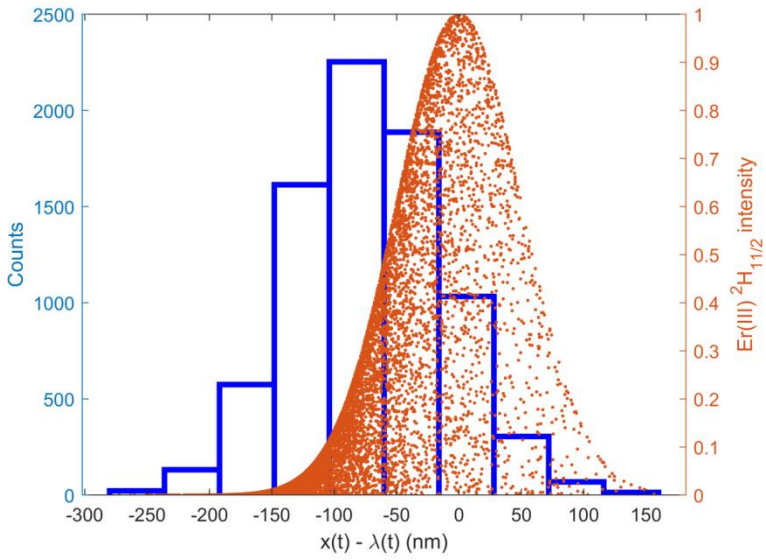

ABSTRACT: Given the remarkable developments in synthetic control over colloidal particle chemical and physical properties, it is interesting to see how stochastic thermodynamics studies may be performed with new, surrogate, or hybrid model systems. In the present work, we apply stochastic dynamics and nonlinear optical light-matter interaction simulations to study non-equilibrium trajectories of individual Yb(III):Er(III) co-doped colloidal and nanoparticles driven by two-dimensional dynamic optical traps. We characterize the role of fluctuations at the single particle level by analyzing position trajectories as well as time-dependent upconversion and downconversion emission intensities. By integrating these two complementary perspectives, we show how the methods developed here can be used to characterize rare events.

INTRODUCTION

The application of fundamental concepts of non-equilibrium statistical mechanics to a variety of small systems (colloidal particles, RNA, DNA, or proteins, among others), has improved our understanding of energy conversion in the microscopic regime (Liphardt et al., 2002; Ciliberto, 2017). Conversely, by treating these systems as the Brownian particle in a Langevin equation description of the underlying dynamics, experimental results have been used to verify theoretical predictions of stochastic thermodynamics, such as fluctuation theorems, the Jarzynski equality, and trajectory entropy (Seifert, 2012). Considering that nowadays it is possible to prepare colloidal particles with varying size, shape, chemical composition, and spectroscopic properties (Chen, 2014; Hueckel et al, 2021), it is interesting to explore such systems in connection with stochastic thermodynamics (Ciliberto, 2017; Bonança and Deffner, 2018; Saha et al., 2021). For example, large, thermal fluctuations can play an important role in individual stochastic realizations of a thermodynamic process, thus motivating the development of experimental methods for enhanced sampling of such rare events.

Previously, we have reported studies of stochastic dynamics and spectroscopy, including upconversion nanoparticles (UCNPs) (Nome et al., 2017a; Oliveira et al., 2019; Oliveira and

Nome, 2020; Cavalcante et al. 2021; Oliveira et al., 2021). In reference (Nome et al., 2017a), we studied stochastic dynamics of co-doped Yb(III):Er(III) UCNPs. Upconversion spectra were used to characterize individual UCNPs, and nonlinear microscopy images based on wavelength-integrated upconversion luminescence were used to quantify stochastic trajectories of individual UCNPs in the presence and absence of optical trapping. The experimental results were compared with Langevin dynamics simulations in the presence of thermal, non-conservative, harmonic, and optical traps. In reference (Oliveira et al., 2021), we studied fundamental light-matter interaction mechanisms in core/triple shell UCNPs from experiments and simulations. Hierarchically structured Nd(III)-Yb(III)-Er(III) UCNPs were excited with CW and femtosecond laser-induced upconversion spectroscopy. The results were compared with light-matter interaction simulations for an 18-level system describing Nd(III)-Yb(III)-Er(III) photophysics over a time range spanning from femtoseconds to real-time.

The stochastic and spectroscopic approaches were combined in reference (Cavalcante et al., 2021) to study how nonlinear optical power laws in Yb(III)-Er(III) UCNPs may be characterized from individual stochastic trajectories in experiments and simulations. We studied UCNPs optically trapped, freely diffusing, and individual particles moving towards the static optical trap. In this way, we showed how stochastic dynamics might be useful for characterizing UCNP photophysics at the single particle level.

In the present work, we propose to study stochastic thermodynamics from a combined spectroscopic/colloidal particle perspective. The combined stochastic-spectroscopic approach is used as a starting point to develop methods for studying how the paradigmatic colloidal particle system of non-equilibrium stochastic thermodynamics is manifested in the nonlinear optical properties of the rare-earth doped colloidal particles. We characterize the role of fluctuations at the single particle level by analyzing position trajectories as well as time-dependent upconversion emission intensities and compare the information content obtained from stochastic and spectroscopic approaches.

RESULTS AND DISCUSSION

The main point of this work is to design an experiment to preferentially study rare events in nonequilibrium stochastic trajectories. It is based on a paradigmatic stochastic thermodynamics system, the single colloidal particle, which here also exhibits a non-linear optical response. In this numerical study, we choose realistic parameters for the setup and system, as described in the Methods section. Optical trapping of upconversion nanoparticles has been described previously for various types of particle shapes and chemical compositions (for example, see Haro-Gonzalez et al., 2013; Ortiz-Rivero et al., 2020; Shan et al., 2021). In statistical physics studies, upconversion nanoparticles have also been used to determine the instantaneous ballistic velocity of a Brownian particle (Brites et al, 2016). Recently, our group has used stochastic dynamics measurements and simulations to calculate power laws from individual upconversion nanoparticles (Cavalcante et al., 2021). Here, we use the power laws to improve the characterization of stochastic trajectories, especially rare events.

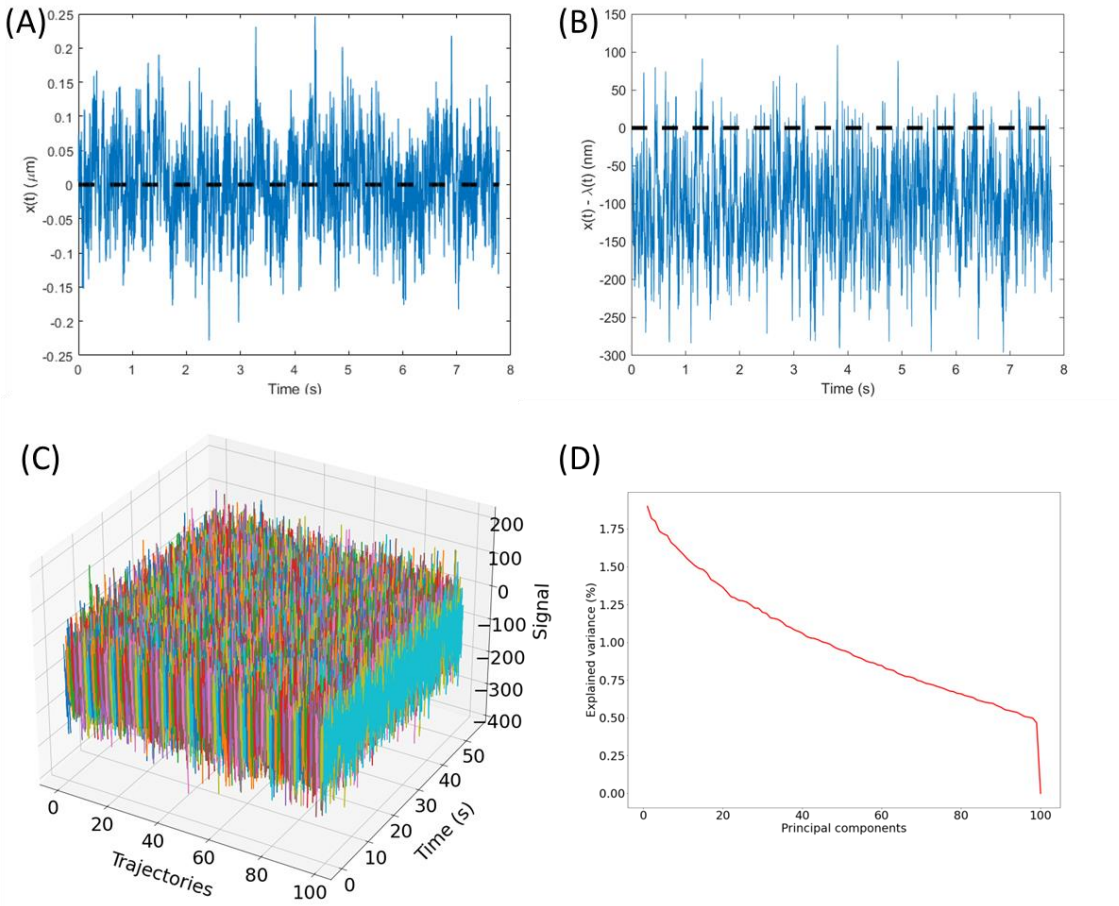

Figure 1. Stochastic trajectories for optically trapped colloidal particle. Simulation parameters: particle radius R = 1 μm, temperature T = 295 K, viscosity of water $\eta = 10^{-3}$ Pa.s, trap stiffness $\kappa_x = \kappa_y = 1$ pN.μm^{-1}. (A) Static optical trap; (B) Dynamic optical trap with pulling velocity v = 1 μm.s^{-1}; (C) Ensemble of 100 independent nonequilibrium trajectories. (D) Principal Component Analysis of the ensemble shown in (C).

Figures 1A and 1B show results of Langevin dynamics simulations of optically trapped colloidal particles with static and dynamic optical traps, respectively. In our control system (Figure 1A), we show the particle position trajectory as a function of time (blue line) when the particle is in the presence of a static optical trap centered at zero (trap center indicated by the dashed black line). As shown in the Supporting Information, the mean and most probable particle position values are located at x = 0, as expected. On the other hand, Figure 1B shows $x(t) - \lambda(t)$ (blue line), which is the difference between x(t), the particle position, and $\lambda(t)$, the center position of the time-dependent harmonic trap. The point where $x(t) - \lambda(t) = 0$ is also shown with a dashed black line to facilitate visual comparison between Figures 1A and 1B. Thus, the trajectory in Figure 1B shows that the average value of the quantity $x(t) - \lambda(t)$ assumes a non-zero value, unlike the control system shown in Figure 1A. In other words, when $x(t) - \lambda(t) < 0$, as shown in Figure 1B, the particle lags the center of the time-dependent trap (Vaikuntanhathan and Jarzynski, 2009). Nonetheless, the histogram associated with this trajectory also follows a Gaussian distribution – see Supporting Information (Seifert, 2012).

We have performed 100 simulations using the same conditions as in Figure 1B, and the resulting trajectories are shown in Figure 1C. Visual inspection of this nonequilibrium ensemble already shows that all trajectories match the behavior observed in Figure 1B. As a check, to look for possible trends in the observed trajectories, we performed principal component analysis (PCA) using the data from the 100 trajectories shown in Figure 1B (Souza and Poppi, 2012). The

results for explained variance by the principal components (Figure 1D) show that no tendencies are present in the data, since these values are extremely low (below 2%). In addition, the loadings analysis of the first three principal components (accumulated variance = 5.51%), presented in the Supporting Information, clearly indicates that the information captured by these three principal components has no preferred variable. Therefore, we can conclude that the trajectories exhibit a Gaussian, uncorrelated stochastic behavior. As an additional consistency check, we have also calculated other stochastic thermodynamic quantities from the individual nonequilibrium trajectories: mean and standard deviation of work and dissipated heat, the associated distributions. These quantities were also used to assess the role of negative work fluctuations on the rare events.

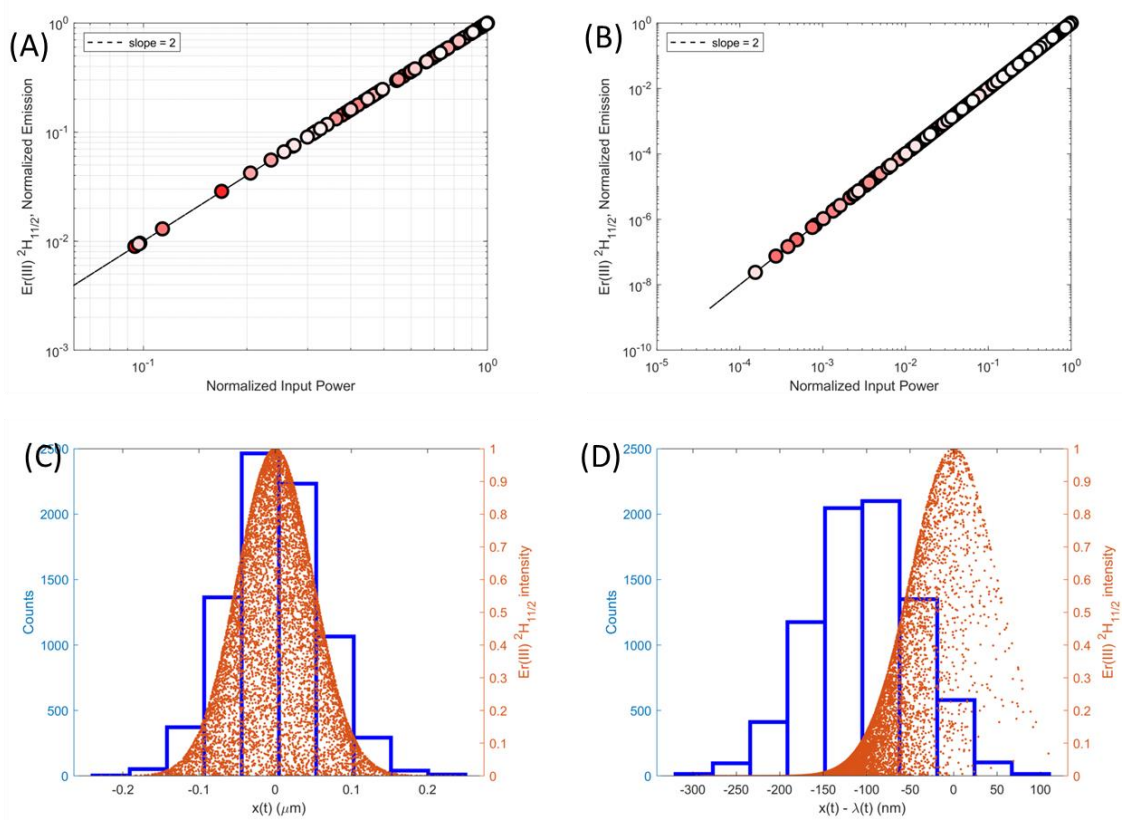

Figure 2. Top: On-the-fly calculation of nonlinear optical power law from individual stochastic trajectories: (A) static optical trap; (B) dynamic optical trap with pulling velocity 1 μm.s^{-1}. The color gradient from red to white represents the simulation time (red corresponds to early time and white corresponds to later time). Bottom: histogram of particle position (in blue) and full set of emission intensities (orange dots) as a function of position: (C) Static optical trap. (D) Dynamic optical trap with pulling velocity 1 μm.s^{-1}. Other simulation parameters are the same as in Figure 1.

In the coupled stochastic-spectroscopic simulations (Sule et al., 2015; Cavalcante et al., 2021), the spatially dependent excitation light intensity distribution is used to probe the Brownian particle optical response. Previously, we used this approach to perform on-the-fly determination of the nonlinear optical power law of upconversion nanoparticles traversing the excitation beam. On the other hand, in the present work, we use the on-the-fly optical response to study stochastic dynamics in a way that complements particle position trajectory-based Zanalysis. To that end, first we characterize the light-matter interaction regime in each simulation condition shown in Figure 1. Figures 2A and 2B show the intensity-dependent upconversion emission power-law calculated on-the-fly from the position trajectories shown in Figures 1A and 1B, respectively. The simulation results are shown with colored circles where the color gradient from red to white represents the simulation time (red corresponds to early time

and white corresponds to later time). In the double logarithmic plots shown in Figures 2A and 2B, the simulation results fall on a straight line, which confirms the power-law equal to two for YbEr. Therefore, for both static (Figure 2A) and dynamic (Figure 2B) optical traps, the Brownian particle can sample lower and higher excitation light intensities at any time, with a nonlinear optical response expected for the YbEr system. In comparing Figures 2A and 2B, we note that a larger intensity range is sampled in the dynamic trap (Fig 2B) due to slope of the Gaussian excitation intensity profile at the center compared to the slope one standard deviation away from the center.

To see the connection between particle location (relative to the trap center) and its intensity more clearly, we combine these two results from the coupled stochastic-spectroscopic approach in Figures 2C and 2D for the static and dynamic traps, respectively. In the case of the static trap, Figure 2C shows an overlap of the particle position histogram (blue) with the distribution of emission intensities (orange dots) of the upconverting particle. As expected for the static trap, the particle spends more time at the center of the trap, which is also where the excitation and upconversion emission intensities are highest. Interestingly, for the dynamic trap, Figure 2D shows that the particle position histogram and the emission intensity distribution peak at different values of the quantity $x(t) - \lambda(t)$. Specifically, the position histogram peaks at $x(t) - \lambda(t) = -100\ nm$ for the simulation parameters in Figure 2D, whereas the emission intensity distribution peaks at $x(t) - \lambda(t) = 0$. Therefore, while the particle spends most of the time in the location consistent with the dynamic harmonic trap pulling protocol, the emission intensity distribution follows the spatial distribution of the excitation light, such that the rare events in the histogram are excited with the highest intensity. Figure 2D is the main result of the present work and illustrates how the integrated stochastic-spectroscopic approach can be used to enhance increase emission intensity of rare events in the nonequilibrium stochastic trajectory.

Finally, we show that the proposed method for spectroscopic detection of rare events in single colloidal particle stochastic thermodynamics may also be realized with other values for the pulling protocol, excitation light, as well as with particle of varying size and chemical composition. For example, Figure 3A shows application of the method using 20 nm radius particles (compare with R = 1 μm in Figures 1 and 2), indicating emission distribution centered at $x(t) - \lambda(t) = 0$ and position histogram centered around $x(t) - \lambda(t) = -300\ nm$. The effect of a smaller trap stiffness of 0.2 $pN.\mu m^{-1}$ (compare with 1 $pN.\mu m^{-1}$ in Figures 1 and 2) is illustrated in Figure 3B, showing emission distribution centered at $x(t) - \lambda(t) = 0$ and position histogram centered around $x(t) - \lambda(t) = -400\ nm$. Figures 3C and 3D compare two different models for upconversion emission based on YbEr and YbTm (Pires et al., 2004; Sigoli et al., 2006; Liang et al., 2021). Both models exhibit nonlinear optical responses that are well characterized with power-law equal to 2 for YbEr and 5 for YbTm, respectively, as shown in Figure 3C. The position histograms (Supporting Information) for YbEr and YbTm overlap and are centered around the same value as before (see Figures 1 and 2). On the other hand, the emission distributions are both centered at $x(t) - \lambda(t) = 0$, although with different shapes, thus clearly illustrating how the optical nonlinearity influences the observation of rare events.

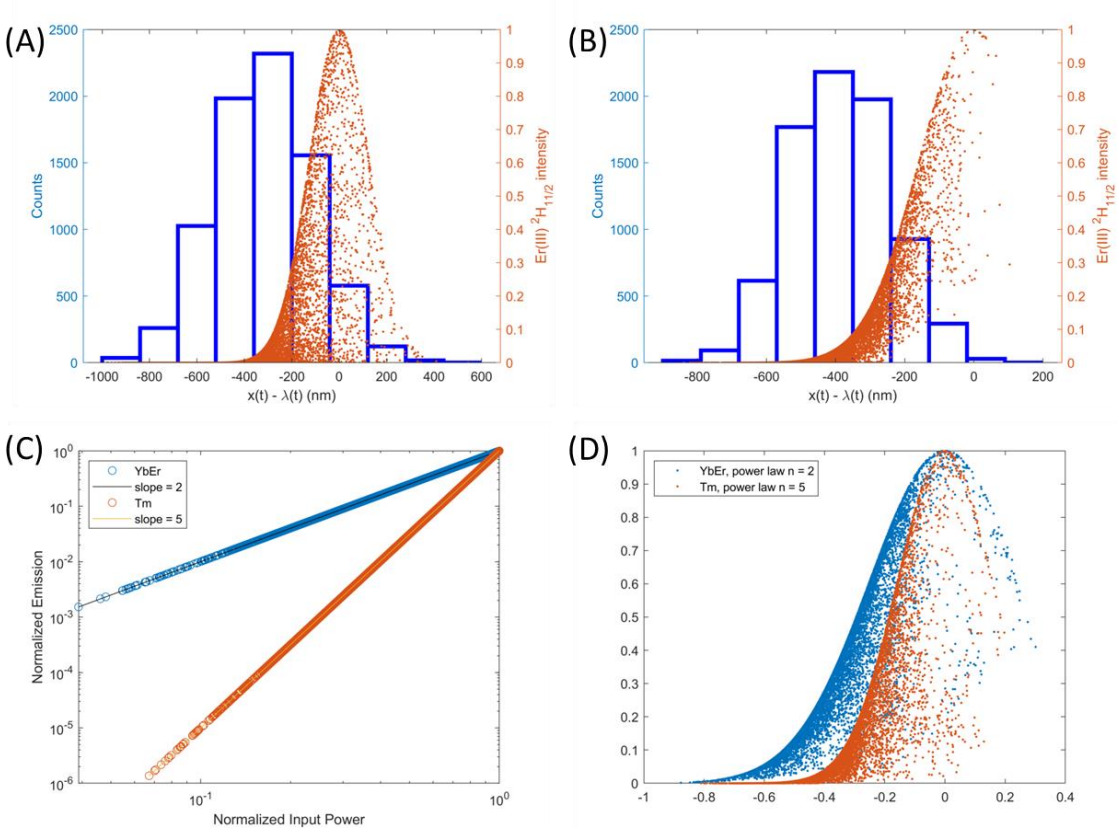

Figure 3. Top: Histogram of particle position (in blue) and full set of emission intensities (orange dots) as a function of position: (A) 20 nm radius nanoparticles in dynamic optical trap; (B) 0.20 pN.μm^{-1} trap stiffness. Bottom: Effect of chemical composition. (C) Nonlinear optical power law for YbEr (blue circles) and Tm (orange circles). (D) Full set of emission intensities for YbEr (blue dots) and Tm (orange dots) as a function of position.

CONCLUSIONS

We have combined stochastic dynamics and nonlinear optical light-matter interaction simulations to study non-equilibrium trajectories of individual particles driven by two-dimensional dynamic optical traps. By integrating these two complementary perspectives, we show how the methods developed here can be used to characterize rare events related to negative work fluctuations. Suggested improvements of this work include using a better model for the spectroscopic system, description of thermal effects, and consider spatial averaging effect. The integrated stochastic-spectroscopic approach may also be extended to study other systems (Nome et al., 2009; Nome et al., 2017b; Ferbonink et al., 2018).

METHODS

For the coupled stochastic-spectroscopic approach, first, we solve the two-dimensional overdamped Langevin equation of motion for a Brownian particle, as described previously (Volpe and Volpe, 2013):

$$\frac{dx(t)}{dt} = \frac{1}{\gamma} F(x) + \sqrt{2D} W_x(t) \quad (1)$$

$$\langle W_x(t) W_x(t') \rangle = \delta(t - t') \quad (2)$$

with friction coefficient γ, diffusion coefficient D, delta-correlated white noise W_x, Boltzmann constant k_B, and temperature T. We study the experimental conditions described in reference (Cavalcante et al., 2021), with particle radius R = 1 μm, temperature T = 295 K, viscosity of water $\eta = 10^{-3}$ Pa.s. The two-dimensional optical trap has trap stiffness $\kappa_x = \kappa_y = 1$ pN.μm^{-1}. The dynamic trap moves linearly in one dimension with pulling velocity v = 1 μm.s^{-1}

$$U\left(x,\lambda\left(t\right)\right) = \tfrac{1}{2}\kappa\left(x-\upsilon t\right)^2 \quad (3)$$

$$\lambda\left(t\right) = \upsilon t \quad (4)$$

The above simulation parameters were used to generate the results shown in Figures 1 and 2. For Figure 3, we also used particle radius R = 20 nm (Figure 3A) and trap stiffness $\kappa_x = \kappa_y$ = 0.2 pN.μm^{-1} (Figure 3B) while keeping the remaining parameters as in Figures 1 and 2.

To describe the spectroscopic properties of the Brownian particle, the rate expressions describing light-matter interactions for the Yb(III)-Er(III) 9 energy-level diagram (Oliveira et al., 2021) are evaluated. In this model, two levels describe Yb(III) and seven levels for Er(III) electronic states, where we model light absorption, non-radiative decay, energy transfer, and radiative emission, as described in refs (Jung et al, 2015; Oliveira et al., 2021; Diogenis et al.). The initial ground-state lanthanide ion populations are parameterized after the experimental chemical composition of the UCNPs, and the remaining spectroscopic constants are as described previously. This energy level diagram was used in the calculations related to Figures 1, 2, 3A, and 3B. For Figures 3C and 3D, we also used the corresponding energy level diagram for the pair YbTm (Pires et al, 2004; Liang et al., 2019).

For the coupled stochastic-spectroscopic dynamics simulations (Sule et al., 2015; Cavalcante et al., 2021), at each time step in the stochastic dynamics simulations, we determine the particle location and the incident light intensity at that location. We assume a two-dimensional Gaussian beam profile for the second, excitation laser, which is used as the excitation source for the spectroscopic transitions. Then, from the particle position and the excitation intensity at that position, we solve the light-matter equations for the Yb(III)-Er(III) energy-level diagram. Steady-state populations for each quantum state are reached on a timescale shorter than the Brownian dynamics time step. Therefore, the steady-state populations calculated at each time step are used as an input for the next iteration during the coupled simulations. The Er(III) $^2H_{11/2}$ population as a function of intensity is calculated on-the-fly as the Brownian particle moves in the presence of the time-dependent field described by equations (3) and (4) above.

FUNDING

RAN acknowledged the support by CNPq INCT Catalysis (grant 444061/20185) and FAPESP (grants 2019/27471-0, 2020/10541-2, and 2020/10518-0). SRM acknowledged the support of FAPESP (grants 2019/27471-0 and 2013/07276-1).

REFERENCES

1. Bonança, M.V.S., Deffner, S. (2018). Minimal dissipation in processes far from equilibrium. Physical Review E 98, 042103, DOI: 10.1103/PhysRevE.98.042103.
2. Brites, C.D.S., Xie, X., Debasu, M.L., Qin, X., Chen, R., Huang, W., Rocha, J., Liu, X., Carlos, L.D. (2016). Instantaneous ballistic velocity of suspended Brownian nanocrystals measured by upconversion nanothermometry. Nat. Nanotech. 11, 851-857, DOI: 10.1038/NNANO.2016.111.
3. Cavalcante, I.N., Marchi, M.C., Sigoli, F.A., de Sousa Filho, P.C., Barja, B.C., Nome, R.A. (2021). “On the fly” evaluation of upconversion nanoparticle power dependence from

individual stochastic trajectories. Optical Manipulation and Its Applications, AW3D. 4, DOI: 10.1364/OMA.2021.AW3D.4
4. Chen, G., Qiu, H., Prasad, P.N., Chen, X. (2014) Upconversion Nanoparticles: Design, Nanochemistry, and Applications in Theranostics. Chem. Rev. 114, 5161-5214. DOI: 10.1021/cr400425h
5. Ciliberto, S. (2017). Experiments in Stochastic Thermodynamics: Short History and Perspectives, Phys. Rev. X 7, 021051, DOI: 10.1103/PhysRevX.7.021051.
6. Diogenis, I.M.S., Rodrigues, E.M., Mazali, I.O., Sigoli, F.A. (2021). Spectroscopic evidence of preferential excitation of interfacial EuIII by interfacial energy transfer process on core@shell nanoparticles. J. Lumin 232, 117848. DOI: 10.1016/j.jlumin.2020.117848
7. Ferbonink, G.F., Rodrigues, T.S., Dos Santos, D.P., Camargo, P.H.C., Albuquerque, R.Q., Nome, R.A. (2018). Correlating structural dynamics and catalytic activity of AgAu nanoparticles with ultrafast spectroscopy and all-atom molecular dynamics simulations. Faraday Discussions 208, 269-286, DOI: 10.1039/C7FD00220C
8. Gieseler, J., Gomez-Solano, J.R., Magazzu, A., Castillo, I.P., Garcia, L.P., Gironella-Torrent, M. et al. (2021). Optical tweezers — from calibration to applications: a tutorial. Adv. Opt. Phot. 13, 74-241. DOI: 10.1364/AOP.394888
9. Haro-Gonzalez, P., del Rosal, B., Maestro, L. M., Martin Rodriguez, E., Naccache, R., Capobianco, J. A., et al. (2013). Optical trapping of NaYF4:Er3+,Yb3+ upconverting fluorescent nanoparticles. Nanoscale 5:12192. DOI: 10.1039/c3nr03644h.
10. Hueckel, T., Hocky, G.M., Sacanna, S. (2021). Total synthesis of colloidal matter. Nat. Rev. Mater. 6, 1053-1069 DOI: 10.1038/s41578-021-00323-x.
11. Jung, T., Jo, H.L., Nam, S.H., Yoo, B., Cho, Y., Kim, J., Kim, H.M., Hyeon, T., Suh, Y.D., Lee, H., Lee, K.T. (2015). The preferred upconversion pathway for the red emission of lanthanide-doped upconverting nanoparticles, NaYF4:Yb3+,Er3+. Phys. Chem. Chem. Phys. 17, 13201. DOI: 10.1039/C5CP01634G
12. Liang, L., Teh, D.B.L., Dinh, N.-D., Chen, W., Chen, Q., Wu, Y., et al. (2019) Upconversion amplification through dielectric superlensing modulation. Nat. Commun. 10: 1391, DOI: 10.1038/s41467-019-09345-0.
13. Liphardt, J., Dumont, S., Smith, S.B., Tinoco Jr., I., Bustamante, C. (2002). Equilibrium Information from Nonequilibrium Measurements in an Experimental Test of Jarzynski's Equality. Science 296, 1832-1835, DOI: 10.1126/science.1071152.
14. Mehlich A., Fang J., Pelz B., Li H., Stigler J. (2020). Slow Transition Path Times Reveal a Complex Folding Barrier in a Designed Protein. Front. Chem. 8:587824. DOI: 10.3389/fchem.2020.587824
15. Nam, S.H., Bae, Y.M., Park, Y.I., Kim, J.H., Kin, H.M., Choi, J.S., Lee, K.T., Hyeon, T., Suh, Y.D. (2011). Long-term real-time tracking of lanthanide ion doped upconverting nanoparticles in living cells. Angew. Chem. 123, 6217-6221. DOI: 10.1002/ange.201007979
16. Nome, R.A., Costa, A.F., Lepkoski, J., Monteiro, G.A., Hayashi, J.G., Cordeiro, C.M.B. (2017). Characterizing slow photochemical reaction kinetics by enhanced sampling of rare events with capillary optical fibers and Kramers' theory. ACS Omega 2, 2719-2727, DOI: 10.1021/acsomega.7b00004.
17. Nome, R.A., Guffey, M.J., Scherer, N.F., Gray, S.K. (2009). Plasmonic interactions and optical forces between Au bipyramidal nanoparticle dimers. J. Phys. Chem. A 113, 4408-4415, DOI: 10.1021/jp811068j
18. Nome, R.A., Sorbello, C. Jobbagy, M., Barja, B. C. , Sanches, V., Cruz, J. S., Aguiar, V. F. (2017). Rich stochastic dynamics of co-doped Er:Yb fluorescence upconversion nanoparticles in the presence of thermal, non-conservative, harmonic and optical forces. Meth. App. Fluor. 5, 014005, DOI: 10.1088/2050-6120/aa5a81.

19. Nome, R.A., Zhao, J.M., Hoff, W.D., Scherer, N.F. (2007). Axis-dependent anisotropy in protein unfolding from integrated nonequilibrium single-molecule experiments, analysis, and simulation. PNAS 104, 20799–20804, DOI: 10.1073/pnas.0701281105
20. Oliveira, G. H., Ferreira, F. S., Ferbonink, G. F., Belançon, M. P., Sigoli, F. A., Nome, R.A. (2021). Femtosecond laser induced luminescence in hierarchically structured NdIII, YbIII, ErIII co-doped upconversion nanoparticles: Light-matter interaction mechanisms from experiments and simulations. J. Lumin. 234, 117953. DOI: 10.1016/j.jlumin.2021.117953
21. Oliveira, G.H., Galante, M.T., Martins, T.T., dos Santos, L.F.L.S., Ely, F., Longo, C. (2019). Real time single TiO2 nanoparticle monitoring of the photodegradation of methylene blue. Solar Energy 190, 239-245. DOI: 10.1016/j.solener.2019.08.006
22. Oliveira, G.H., Nome, R.A. (2019). Integrating ultrafast and stochastic dynamics studies of Brownian motion in molecular systems and colloidal particles. Curr. Op. Coll. & Int. Sci. 44, 208-219. DOI: 10.1016/j.cocis.2019.11.002
23. Ortiz-Rivero, E., Labrador-Paéz, L., Rodríguez-Sevilla, P., Haro-González, P. (2020). Optical Manipulation of Lanthanide-Doped Nanoparticles: How to Overcome Their Limitations. Front. Chem. 8, 593398, DOI: 10.3389/fchem.2020.593398.
24. Pires, A.M., Serra, O.A., Davolos, M.R. (2004). Yttrium oxysulfide nanosized spherical particles doped with Yb and Er or Yb and Tm: efficient materials for up-converting phosphor technology field. Journal of Alloys and Compounds 374, 181-184, DOI: 10.1016/j.jallcom.2003.11.088
25. Seifert, U. (2012). Stochastic thermodynamics, fluctuation theorems and molecular machines. Rep. Prog. Phys. 75, 126001, doi:10.1088/0034-4885/75/12/126001.
26. Shan, X., Wang, F., Wang, D. et al (2021). Optical tweezers beyond refractive index mismatch using highly doped upconversion nanoparticles. Nat. Nanotechnol. 16, 531–537, DOI: 10.1038/s41565-021-00852-0.
27. Sigoli, F. A., Gonçalves, R. R. , Messaddeq, Y., Ribeiro, S. J. L. (2006). Erbium- and ytterbium-doped sol–gel SiO2–HfO2 crack-free thick films onto silica on silicon substrate, J. Non-Cryst. Solids, 352, 3463-3468, DOI: 10.1016/j.jnoncrysol.2006.03.081
28. Sousa Filho, P.C., Alain, J., Leménager, G., Larquet, E., Fick, J., Serra, O.A., Gacoinde, T. (2019) Colloidal rare earth vanadate single crystalline particles as ratiometric luminescent thermometers. J. Phys. Chem. C 123, 2441-2450. DOI: 10.1021/acs.jpcc.8b12251.
29. Souza, A.M., Poppi, R.J. (2012). Experimento didático de quimiometria para análise exploratória de óleos vegetais comestíveis por espectroscopia no infravermelho médio e análise de componentes principais: um tutorial, parte I. Química Nova 35, 223-229, DOI: 10.1590/S0100-40422012000100039.
30. Sule, N., Rice, S.A., Gray, S.K., Scherer, N.F. (2015) An electrodynamics-Langevin dynamics (ED-LD) approach to simulate metal nanoparticle interactions and motion. Opt. Exp. 23, 29978-29992, DOI:10.1364/OE.23.029978
31. Saha, T. K., Lucero, J.N. E., Ehrich, J., Sivak, D. A., Bechhoefer, J. (2021). Maximizing power and velocity of an information engine. Proc. Natl. Acad. Sci. U.S.A. 118, e2023356118. DOI:/10.1073/pnas.2023356118
32. Vaikuntanathan, S., Jarzynski, C. (2009). Dissipation and lag in irreversible processes. EPL 87, 60005. DOI: 10.1209/0295-5075/87/60005.
33. Volpe, G., Volpe, G. (2013). Simulation of a Brownian particle in an optical trap. Am. J. Phys. 81, 224, DOI: 10.1119/1.4772632.